LHC Project Note 312

2003-02-19

Thierry.Boutboul@cern.ch

Low-current Resistance of Multifilamentary Superconducting Cu/NbTi Strands

T. Boutboul, P. Lezza and R. Wolf / AT-MAS-SC

Keywords: superconductors, NbTi, critical current, self-field

Summary

We report on low-current resistance data of NbTi superconducting strands measured at CERN, for several strand types and as a function of important parameters like temperature, applied magnetic field and current ramp rate. The observed dynamic resistance can be well understood by the transport current penetration into the strand during the measurement.

1 Introduction

The critical current of the multifilamentary superconducting Cu/NbTi strands composing the Rutherford-type cables for LHC dipoles and quadrupoles is currently measured at CERN, at both 4.2 K and 1.9 K. More than 6000 strand samples have already been tested to qualify the LHC strand production. Experimental setup and procedures of these measurements were already presented in [1]. A typical voltage-current curve, as recorded during a critical current measurement, is shown in Fig. 1.

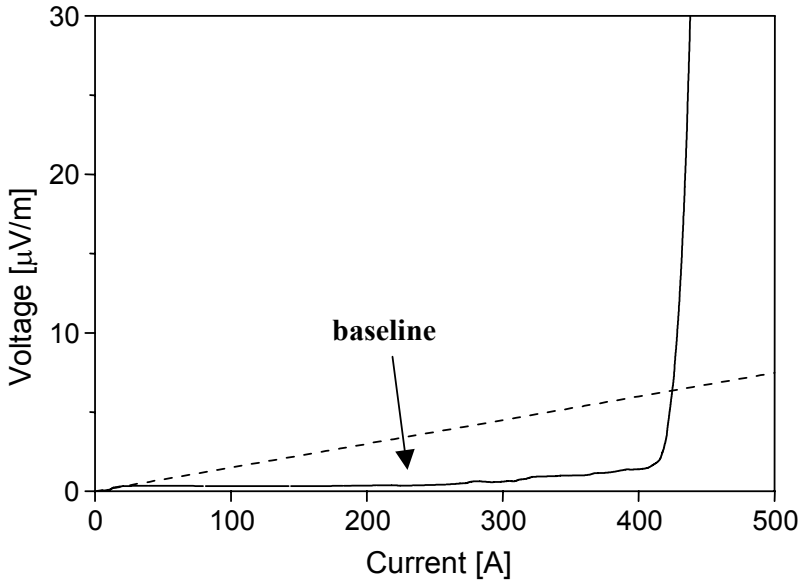

Fig. 1. A typical V-I curve for a superconducting Cu/NbTi strand of LHC dipole outer layer cable. This measurement was done at 1.9 K and 9 T. The dashed line corresponds to 10^{-14} Ω·m total section resistivity criterion for critical current. The critical current value is 426 A.

An interesting issue appearing in such measurements is that the slope of the voltage baseline is not zero as expected, even far from transition (i.e. for currents substantially below the critical current value). The resulting overall resistance is typically of a few nΩ. This phenomenon, also observed at other laboratories [2], is generally explained in literature by a current transfer effect [3],[4]. Indeed, close to the input current lead, the current penetrates through the matrix material (copper in our case) before reaching the superconducting filaments. Nevertheless, at CERN apparatus, the distance between the input lead and the first voltage tap is around 20 cm, i.e. much more than the current transfer length as estimated by Ekin [3] (typically a few mm for LHC-type strands). Therefore, the current transfer could not explain the baseline resistance effect. In V-I measurements, the current should be increased with a constant rate. Therefore the current ramp linearity was checked. The typical deviation from linearity could only induce a resistance of several pΩ and thus it could not cause the mentioned phenomenon. Thus it appears that the baseline resistance issue is a genuine problem and it needs further investigation.

In the present work, we report on low-current resistance data as measured at CERN, for several strand types and as a function of important parameters like temperature, applied magnetic field and current ramp rate. Afterwards, a calculation model is proposed to elucidate the phenomenon.

2 Experimental work

Details about the experimental setup and procedures of CERN critical current measurements can be found in [1]. The tested strands are mounted onto a cylindrical holder and the distance between the voltage taps is 80 cm. At given conditions of temperature and external magnetic field, the critical current (I_c) is measured by increasing the current flowing through the strand sample with a linear ramp (12.5 A/s in standard tests). The I_c value is evaluated according to the 10^{-14} Ω.m total section resistivity criterion.

The low-current or baseline resistance (BR) is derived by determining the slope of the V-I curve between 10 % and 90 % of this I_c value. It should be stressed that BR measurements present serious fluctuations, the reproducibility being typically within dozens of percents. This is due to the fact that voltages within the baseline range are of the order of a μV, the signal-to-noise ratio thus being of a few units in this range. Therefore, in order to provide representative BR experimental data, it is crucial to average over several measurements.

2.1 Influence of the measurement setup and strand manufacturer

The first step was to check whether there is any link between the BR value and the specific system in which it was measured. For this purpose, the baseline slope data as recorded at CERN during one-year I_c measurements were considered, in the case of 0.825 mm in diameter wires used for the outer layer cables of LHC dipoles and quadrupoles [1], as supplied by four manufacturers. Those critical current tests were performed on several hundreds of strand samples and on various test stations (4), sample holders (8) or sample inserts (8). These measurements were sorted out according to the used test station, sample insert and sample holder. It appears that there is no correlation between the low-current resistance and the experimental apparatus. Furthermore, the same data appeared to be also not correlated to the strand manufacturer, the four strand makers providing wires with BR values that were quite comparable.

2.2 Temperature and magnetic field effect

Afterwards, the one-year I_c database, mentioned above, was considered in order to examine the temperature and magnetic field dependence of the baseline slope. Fig. 2 shows the BR as a function of external applied field for both 1.9 K and 4.3 K. All the measurements were performed with a current ramp of 12.5 A/s, as already mentioned. In Fig. 2, every BR datum is the average of about 300 measurements for strands tested in the specific station, sample insert and sample holder. Thus it appears that the magnetic field dependence of BR is quite linear for considered temperatures. In both temperature cases, the low-current resistance seems to be an increasing function of field. It is also interesting to note that 4.3 K and 1.9 K curves are quite parallel lines with a shift of 3-3.5 T.

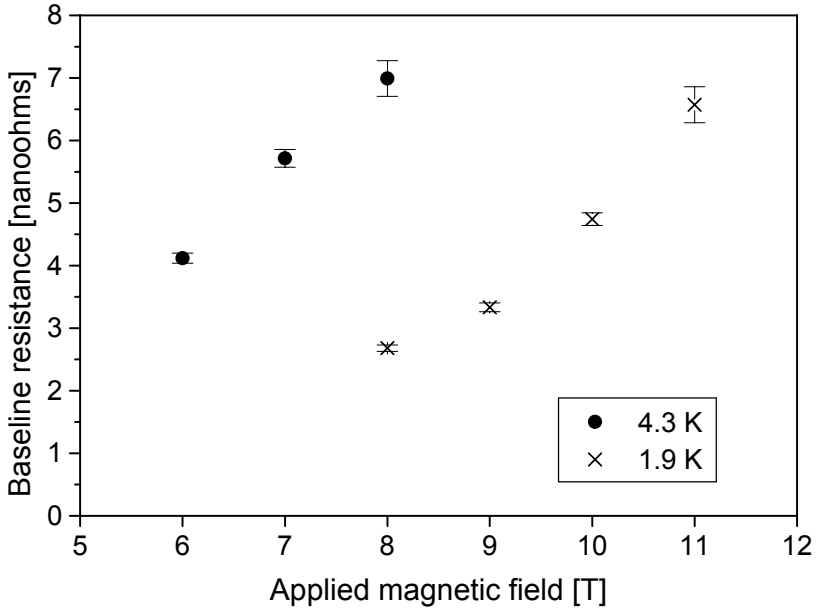

Fig. 2. The baseline resistance as averaged over one-year CERN measurements of LHC dipole outer layer cable strands and as a function of the applied magnetic field for 4.3 K and 1.9 K (see text). Error bars show the statistical uncertainty in the average.

2.3 Low-current resistance dependence on current ramp rate

The effect of the current ramp on the BR was investigated. For this purpose, the low-current resistance was estimated for two strands of different kinds, A_0 and B_0. Strand A_0 is a 1.065 mm in diameter wire used in the inner layer cables of LHC dipoles. Strand B_0 is similar to outer layer cable dipole strands exhibited in Fig. 2 (0.825 mm in diameter). For the sake of statistics, every BR datum presented in Fig. 3-Fig. 5 is the baseline slope average of, at least, five measurements. Fig. 3 shows the resistance data versus current ramp, for strand A_0, as measured at 1.9 K and 9 T.

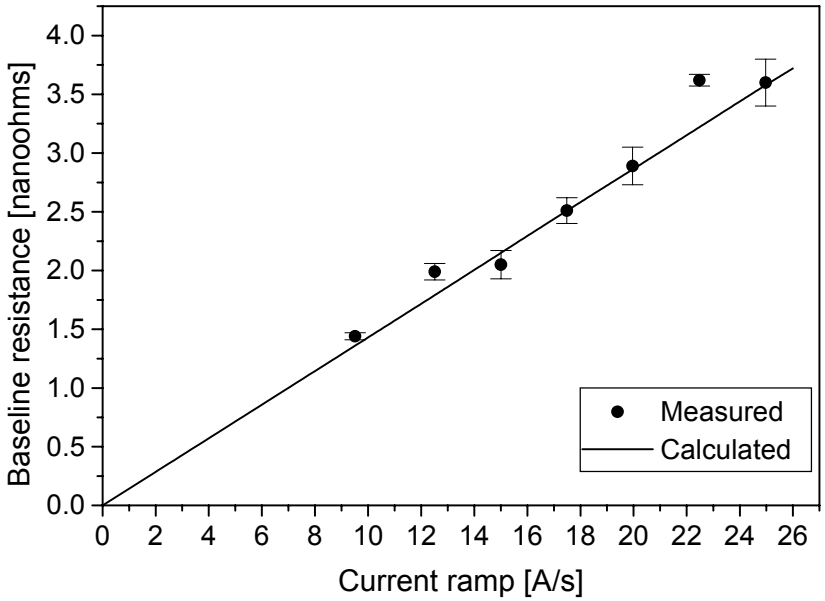

Fig. 3. The baseline resistance of strand A_0 versus current ramp, as measured at 1.9 K and 9 T (symbols). The full line represents calculated values.

Fig. 4 and Fig. 5 present the BR values in the case of strand B_0, at 1.9 K and under an applied field of 8 and 11 T respectively.

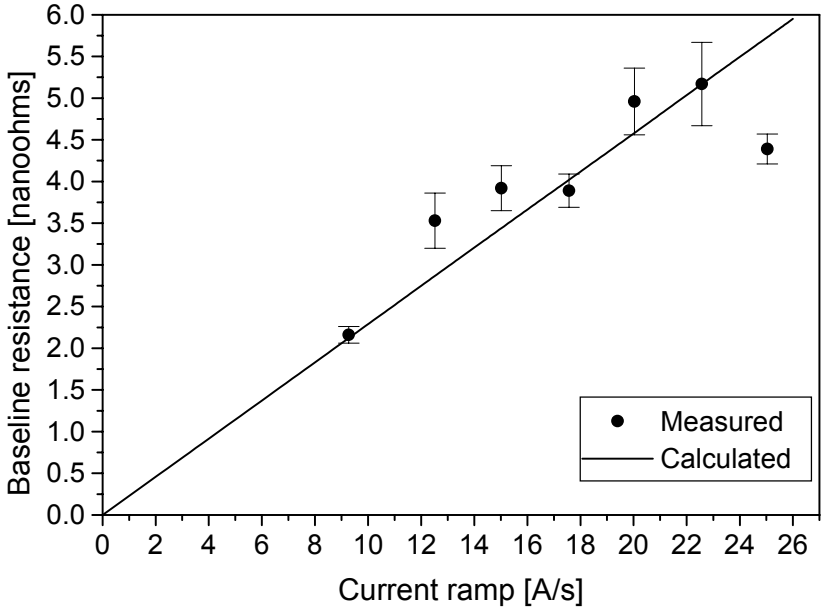

Fig. 4. The baseline resistance of strand B_0 versus current ramp, as measured at 1.9 K and 8 T (symbols). The full line represents calculated values.

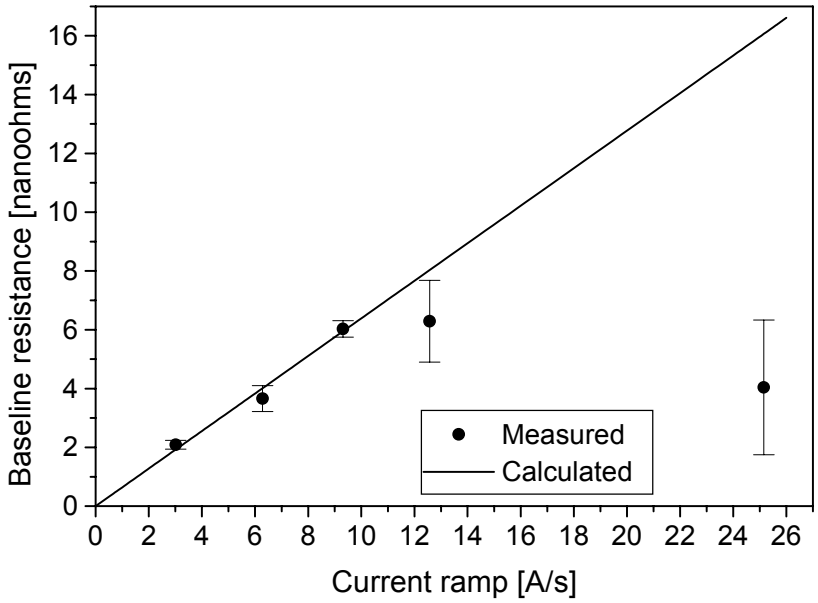

Fig. 5. The baseline resistance of strand B_0 versus current ramp, as measured at 1.9 K and 11 T (symbols). The full line represents calculated values.

As clearly shown by Fig. 3-Fig. 5, the BR values present a quite linear dependence in current ramp, except for strand B_0, at 11 T and current ramp of 25 A/s (see Fig. 5). Fig. 3-Fig. 5 also suggest that a linear extrapolation to zero ramp provides nil resistance. The zero ramp case was considered by means of "point-by-point" measurements. For this purpose, the current was increased and stabilized and then the voltage was recorded. This was done on a B_0 strand sample at 1.9 K and 9 T, where around twenty data were measured between 10 and 90 % of the critical current value (i.e. between ~ 40 and ~ 380 A). The baseline resistance was found to be typically zero, at least less than 0.2 nΩ, thus confirming the hypothesis.

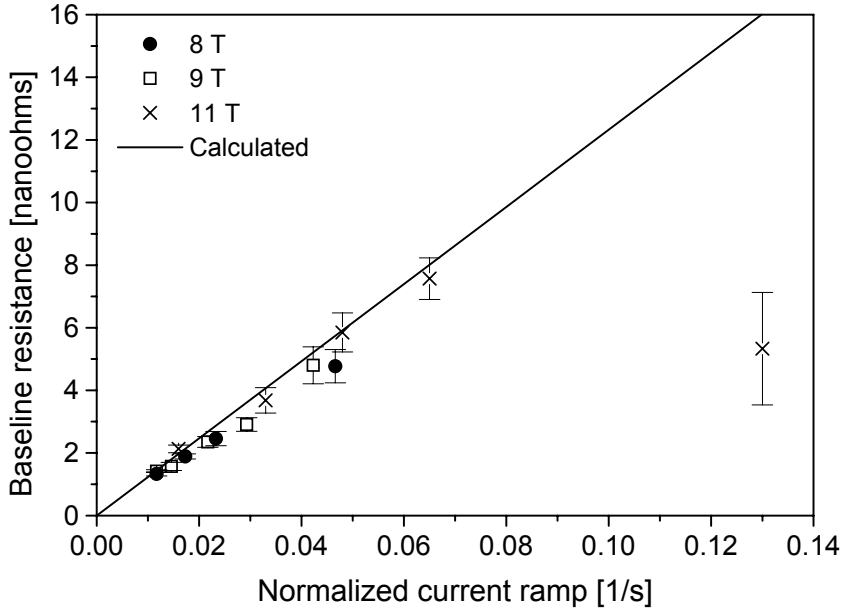

Fig. 6. The baseline resistance of strand B_0, as measured at 1.9 K and 8, 9 and 11 T, versus the current ramp as normalized to critical current. The full line represents calculated values.

The 3-3.5 T shift between 1.9 K and 4.3 K BR versus field curves, as shown in Fig. 2, reminds us of a similar shift (~ 3 T [5]) for critical current values as measured under various values of magnetic field and between the mentioned temperatures. The BR dependence on temperature and field could be only due to I_c link to both latter factors. Therefore, it was rather interesting to verify the BR dependence on $(dI/dt)/I_c$, i.e. the current ramp as normalized to critical current or the superconductor current filling rate. The low-current resistance was thus measured on a B_0 strand sample, at 1.9 K and 8, 9 and 11 T, for several current ramps. The BR value, as averaged over five measurements, is presented in Fig. 6 as a function of the normalized current ramp.

As shown by Fig. 6, the linear BR dependence on the superconductor-filling rate is quite impressive, except in the case of 0.13 s^{-1} datum. In order to verify this linear trend more systematically, the critical current curves of three samples, as recorded for magnetic fields and temperatures respectively within the 3-12.5 T and 1.8-4.3 K ranges, were considered. These measurements, done at the constant current ramp of 12.5 A/s, were performed for A_1 and for B_1 and B_2 strand samples that are similar to A_0 and B_0 wires respectively.

Fig. 7-Fig. 9 show the BR values as averaged over nine measurements for each couple of field and temperature conditions (see the respective figure captions for more details).

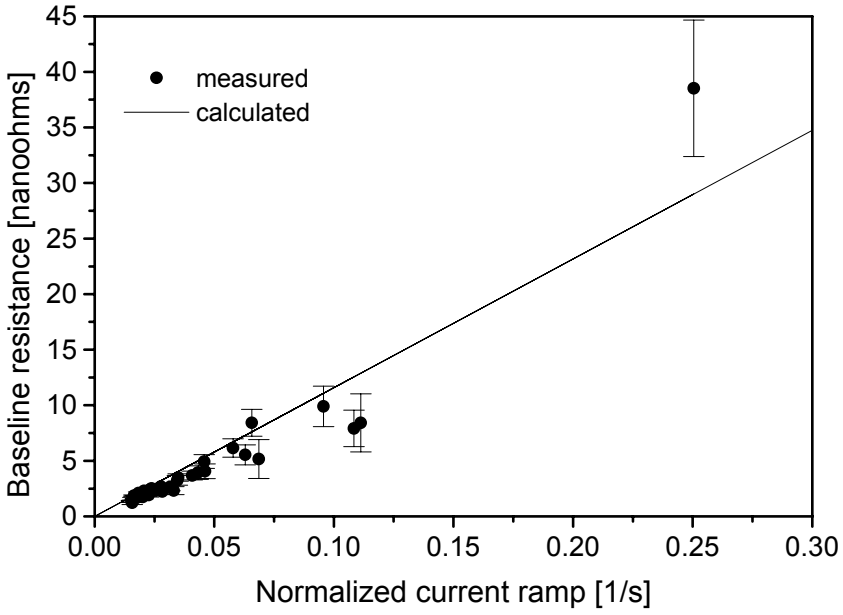

Fig. 7. The baseline resistance data of strand A_1 as a function of normalized current ramp, for temperature and applied magnetic field conditions: 1.8 K and 1.9 K (8.5-12.5 T range), 2 K (8.5-12 T) and 4.3 K (5.5-10 T).

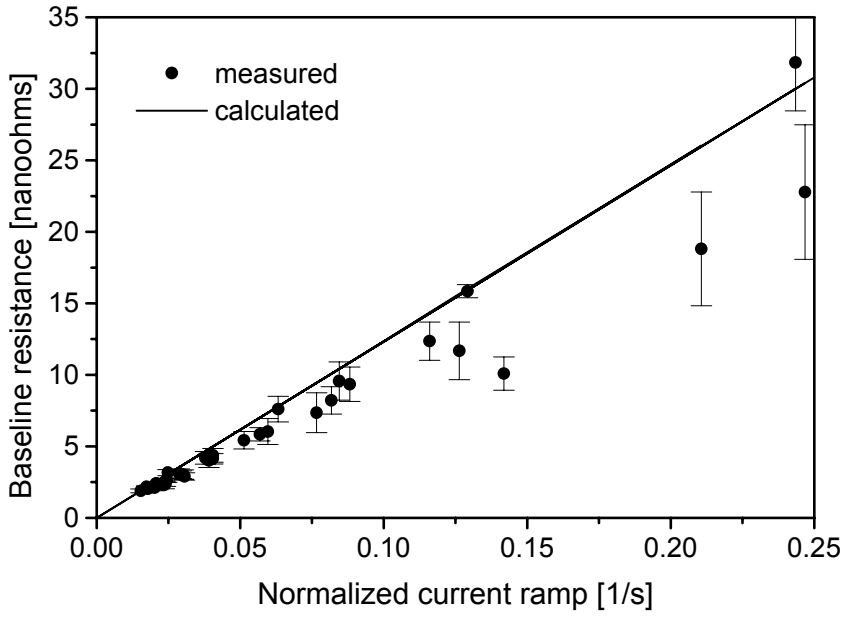

Fig. 8. : Same as Fig. 7 for strand B_1 and conditions: 1.8 K (6-12.5 T), 1.9 K (5-12.5 T), 2 K (6-12 T) and 4.3 K (3-9.5 T).

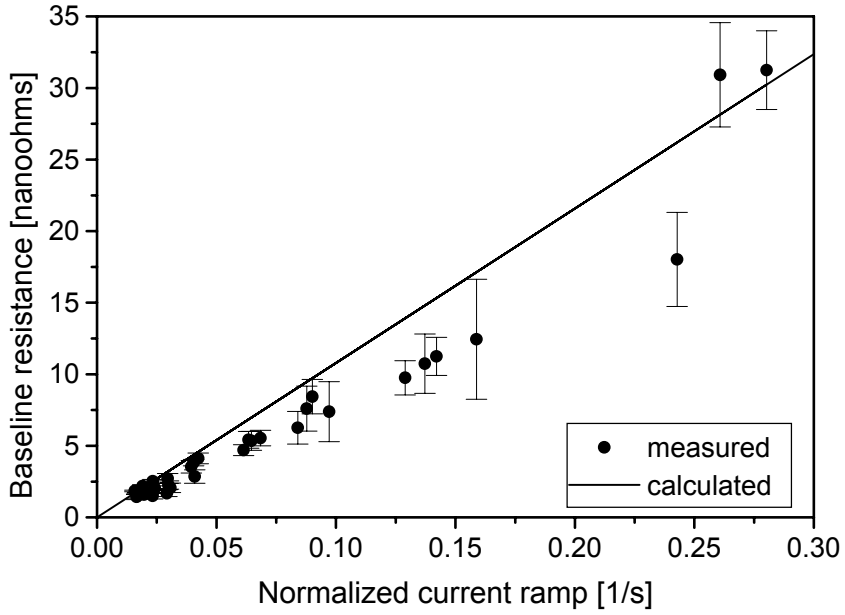

Fig. 9. Same as Fig. 7 for strand B_2 and conditions: 1.8 K and 1.9 K (6-12.5 T), 2 K (6-12 T) and 4.3 K (3-9.5 T).

For the three mentioned samples, the low-current resistance also appears to be a quite linear function of normalized current ramp, at least for low ramp values (i.e. less than 0.1 s^{-1}). It is rather remarkable that this feature is common to three various samples, for a broad range of temperatures and applied magnetic field values.

In the next section, a calculation model will be proposed to explain the linear BR dependence on normalized current ramp.

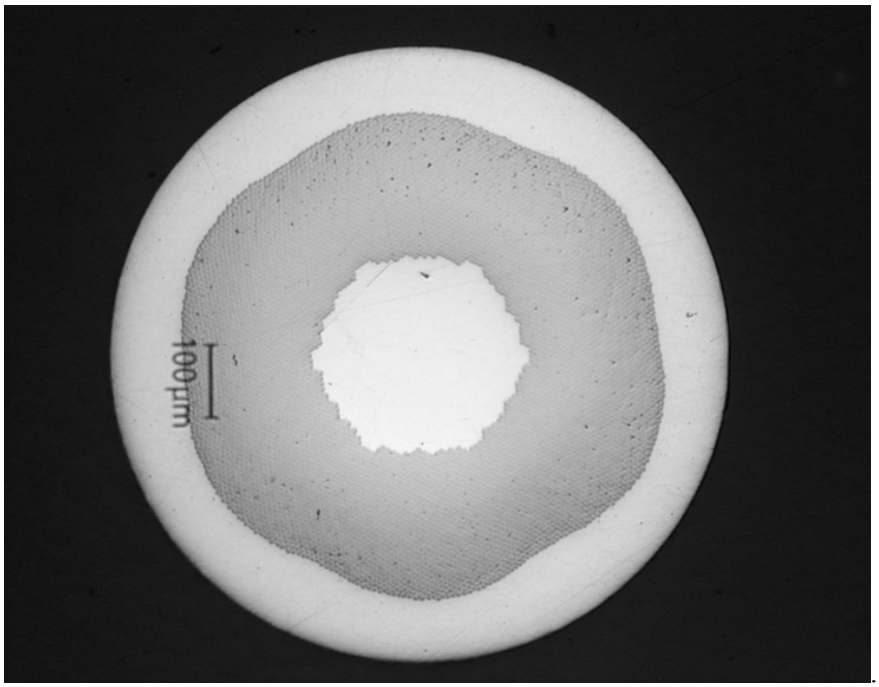

Fig. 10. A microscope view of the cross-section of a typical LHC superconducting strand (for dipole outer layer cable). A composite Cu/NbTi area (in grey) is embedded between two copper regions (the external crown and the internal core).

3 Calculation model

A cross-section microscope view of a typical LHC superconducting strand is presented in Fig. 10. Such a conductor is composed of three different regions: an external copper ring, an internal copper core and a composite Cu/NbTi area between them. In this intermediate region, the NbTi filaments are embedded within a copper matrix. Although the current is fed to the conductor through the outer Cu region, the current transfer through it can be neglected in our considerations since the first voltage tap is far enough from the input current lead, as already explained above. In this model, the composite area will be considered as a homogeneous superconducting medium, characterized by a constant critical current density, J_c, and a superconductor filling ratio, λ (typically 0.6-0.7). The superconducting strand will be assumed to be a straight wire with straight NbTi filaments, thus neglecting both helical wire shape (due to sample holder form) and filament twist. These assumptions will be discussed in next section. The proposed approach is based on the Critical State Model, similarly to [6],[7]. Therefore, the current density within the strand is assumed to be either J_c or zero, depending whether current is flowing or not. At a given time t, the current is thus given by the following expression:

$$I = \lambda\pi(r_2^2 - r_p^2)J_c \tag{1}$$

and the critical current is:

$$I_c = \lambda\pi(r_2^2 - r_1^2)J_c \tag{2}$$

where r_1 and r_2 are respectively the inner and the outer radius of the NbTi/Cu composite ring and r_p is the radius to which the current penetrates. r_p can be derived from equations (1) and (2):

$$r_p = \sqrt{r_2^2 - \frac{I}{I_c}(r_2^2 - r_1^2)} \tag{3}$$

Since the filament twist is neglected, the magnetic self-field due to the transport current has only an azimuthal component given by:

$$B_{SF} = \frac{\mu_0 I_r}{2\pi r} \tag{4}$$

or

$$B_{SF} = \frac{\mu_0 \lambda}{2r} J_c (r^2 - r_p^2) \tag{5}$$

for $r \geq r_p$, I_r being the current enclosed between radii r_p and r.

The electric field induced by the current linear change and by the current penetration following it is given by Maxwell's equation:

$$\nabla \times \vec{E} = -\frac{\partial \vec{B}}{\partial t} \tag{6}$$

where $\vec{B}$ is the sum of the constant external magnetic field and $\vec{B}_{SF}$.

Since the voltage taps are far from the input current lead, the longitudinal dependence of the radial electric field component can be neglected. Then, (6) can be written as:

$$\frac{\partial E_z}{\partial r} = \frac{\partial B_{SF}}{\partial t} \tag{7}$$

Deriving (4) and inserting into (7):

$$\frac{\partial E_z}{\partial r} = \frac{\mu_0}{2\pi r} \frac{dI}{dt} \tag{8}$$

Thus:

$$E_z = \frac{\mu_0}{2\pi} \frac{dI}{dt} \ln r + cst \tag{9}$$

Since E_z is zero for r less than r_p, and should be continuous through $r = r_p$, the longitudinal electric component is thus given, for $r \geq r_p$, by:

$$E_z = \frac{\mu_0}{2\pi} \frac{dI}{dt} \ln(r / r_p) \tag{10}$$

At a given transport current, the voltage, as measured on the strand surface ($r = a$) and between two voltage taps separated by a distance l_0, is given by:

$$|\Delta V| = \frac{\mu_0}{2\pi} l_0 \ln(a / r_p) \frac{dI}{dt} \tag{11}$$

where a is the strand radius and r_p is defined by (3). The voltage increase as a function of the current is then:

$$|\Delta V - \Delta V(I = 0)| = -\frac{\mu_0}{4\pi} l_0 \ln\left[1 - \frac{I}{I_c}\left(1 - \frac{r_1^2}{r_2^2}\right)\right] \frac{dI}{dt} \tag{12}$$

It is rather remarkable to note that the voltage increase and then the subsequent baseline resistance, $R_{b.l.}$, depend on the strand internal structure, as expressed by r_1 and r_2, and not on the strand radius where voltage taps are located.

A rough approximation of the baseline resistance can easily be estimated by calculating the slope on the basis of both extreme data (i.e. $I/I_c = 0.1$ and $I/I_c = 0.9$):

$$R_{b.l.} \cong \frac{\mu_0 l_0}{2\pi} \frac{\ln[r_p(0.1) / r_p(0.9)]}{0.8} \frac{dI/dt}{I_c}. \tag{13}$$

However, in order to more accurately compare the model with experimental data, the calculated $R_{b.l.}$ was determined using the best linear fit to the voltage (12) between $I/I_c = 0.1$ and $I/I_c = 0.9$. This direct method was used for all the calculations performed in the present study. Nevertheless, the BR values calculated in such a way are similar to those approximated according to (13) within a few percents. It should be pointed out that the voltage-current curve does not exhibit, in general, a very linear behaviour. This can easily be deduced from (12) where the linearity of the logarithmic term in I is well established only when $r_1 \approx r_2$. This is obviously not the case for most of the samples presented here (see Table 1). The statistical uncertainty of the calculated baseline resistance, due to V-I linear fit error, is typically 4 %.

4 Comparison of the model with measurements

Table 1. The main parameters used in the calculations for all the strands considered in this work. For each wire kind, the strand radius, the inner and outer radii of the NbTi/Cu composite area and the volume superconductor-filling ratio are summarized.

Strand	a [mm]	r_1 [mm]	r_2 [mm]	λ
A_0	0.533	0.198	0.447	0.67
A_1	0.532	0.195	0.448	0.65
B_0	0.413	0.133	0.322	0.67
B_1	0.413	0.149	0.330	0.67
B_2	0.413	0.166	0.343	0.65
C	0.235	0.100	0.193	0.74
D_0	0.350	0.269	0.306	0.76

The BR calculated values were already presented in section 2, together with the corresponding experimental data. The main parameters used in the calculations are shown in Table 1, for all the strand samples considered in this work. r_1 and r_2 parameter values were obtained by examining strand cross-section micrographs (as in Fig. 10).

As shown by Fig. 3-Fig. 5, for strands A_0 (1.9 K and 9 T) and B_0 (1.9 K, 8 and 11 T), it appears that the model-calculated low-voltage resistances agree fairly well with the BR data measured as a function of the current ramp, except for 25 A/s ramp (see Fig. 4 and more especially Fig. 5). When verifying the model consistency in the case of BR dependence on normalized current ramp, the calculated values seem to be quite consistent with experimental data for samples B_0, A_1 and B_1 and for low normalized current ramps (up to ~ 0.1 s^{-1}), as shown by Fig. 6-Fig. 8. However, it appears that the predicted BR values are slightly overestimated as compared to measured data. This trend is even more noticeable in the case of B_2 sample, for which the overestimation reaches tens of % even for low normalized ramps, as shown in Fig. 9.

As an additional test of the proposed model, experimental BR data were compared to calculated results in the case of superconducting Cu/NbTi strands that will be used in the LHC insertion quadrupole magnets. These strands, ~ 0.5 mm in diameter, are thinner than wires previously considered in this work; their characteristics can be found in Table 1 (see strand C). The experimental low-current resistances, as measured during standard CERN tests (12.5 A/s), were averaged over all the tested samples (around 20) for both 4.3 K and 1.9 K and for magnetic fields in the 4-9 T range. These BR values were compared to those predicted by the model. Experimental data and model-based calculations are presented in Fig. 11. It appears that both measured and calculated resistances are fairly similar within a few % for all temperature and field conditions, the maximal deviation between them being 11 %. The normalized current ramps were in the 0.06-0.08 s^{-1} range.

Finally, the model was probed for a strand used in magnetic resonance applications and composed of a unique layer of thick (~ 40 μm in diameter) filaments (see strand D_0 in Table 1). The measured BR data, as averaged over five current ramps, and the predicted values were found to be similar, i.e. in the 1-2 nΩ range, for all the considered temperature and field conditions (4.3 K and 1.9 K, 2-8 T).

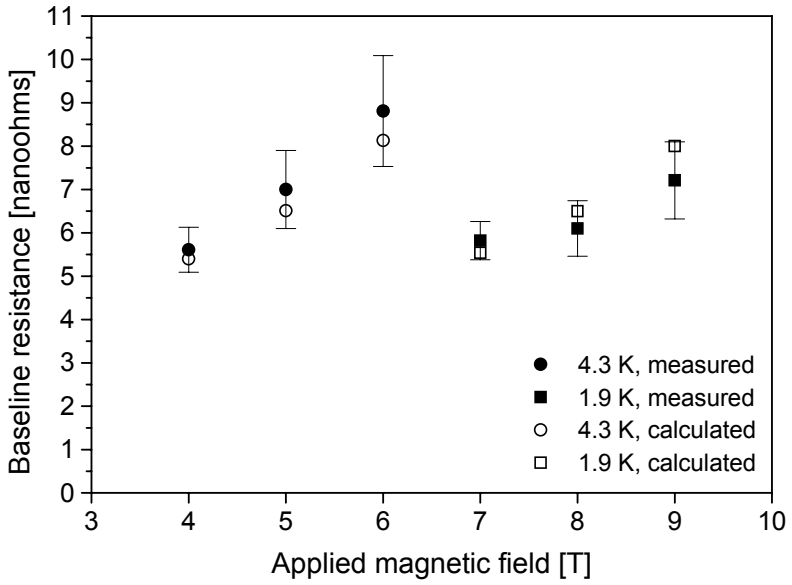

Fig. 11. The experimental low-current resistances (full symbols) as averaged over ~ 20 C-type strands and as a function of magnetic field for 4.3 K (circles) and 1.9 K (squares). Hollow symbols represent model-calculated values for 4.3 K (circles) and 1.9 K (squares).

5 Discussion

5.1 Sample holder shape and twist pitch

In the framework of the model presented in the previous section, the superconducting strand was assumed to be a straight wire and the NbTi filament twist was neglected. Since both sample holder diameter (82 mm) and the spacing between adjacent strand turns (28 mm) are much larger than the strand diameter (~ 1 mm), considering the holder-mounted strand as a straight conductor seems to be a sound approximation. This assumption is supported by numerical self-field calculations, based on Biot-Savart law, that predict for our holder configuration self-field values similar within a few percent to those of an infinite straight conductor, for both inner and outer layer LHC strands.

Concerning neglected filament twist, one should stress that the twist pitch (typically 15-20 mm for all strands considered in this work) is much larger than the dimensions of the Cu/NbTi composite area (~ 0.2 mm). In such a case, the twist effect can easily be neglected and therefore the filaments can be approximated to be straight. This assumption was furthermore confirmed by comparing measured baseline resistance values for both twisted and untwisted samples, as taken from the same strand piece length. No substantial difference indeed appeared between resistances for both samples and for various current ramps. Moreover, the low-current resistance was measured to be quite independent of the sample twist pitch in the 4-13 mm range.

5.2 Shape of the resistive transition.

The calculation model is based on the critical-state model assumption of an infinitely sharp resistive transition at J_c, providing the current density being either 0 or J_c. In fact, the resistivity behaves according to the well-known power law (~ $(J/J_c)^n$). However, it is known that the critical-state model provides a fair representation of the current density distribution in the case of n of the order of a few dozens (see for example [8]), n being in the 30-50 range for the considered strands.

5.3 Matrix resistivity

A major drawback of the model is that it does not account for the matrix material. Indeed, the composite NbTi/Cu area is considered as a homogeneous superconducting medium with a volume superconducting filling ratio. In fact, the matrix resistivity can have a substantial effect on current redistribution within filaments due to their deformed cross-section. This resistivity can also affect the current penetration

towards inner filaments and then have an impact on low-current resistance. The matrix material effect was considered by measuring the baseline resistance for similar strands with either Cu or CuMn matrix. Although CuMn resistivity is higher than that of Cu by three orders of magnitude, both strands exhibited quite consistent resistance values for given normalized current ramps. Therefore neglecting the matrix effect and then considering the composite region as homogeneous seems to be a sound approximation for the strands investigated in this work. This could be explained by the fact that the inter-filament spacing (typically 1 μm) is substantially smaller than filament diameter (~ 6-7 μm).

6 Conclusion

The presented model evaluates the voltage induced by the self-field variation due to current penetration into the inner superconducting filaments. Despite its simplicity, the model provides low-current resistance estimates quite similar to the measured data for wires of various internal structures and for a wide range of temperature, magnetic field and current ramp conditions, except in the case of B_2 strand (see Fig. 9). It is rather interesting to note that the measured baseline resistance is proportional to the current ramp as normalized by the critical current, i.e. the strand current filling rate. This feature is obviously predicted by the model. Therefore, it appears that the low-current resistance, observed during critical current measurements, is caused by the self-field change following the current increase and then its penetration within inner filaments. Further efforts should be invested to refine the model, for accounting for matrix and current redistribution effects.

7 Acknowledgments

The authors would like to thank D. Leroy for motivating this research and for his strong support. They thank A.K. Ghosh (BNL) for providing strand samples and very useful discussions and L. Oberli for very helpful discussions. The authors thank L. Rossi, J.-L. Duchateau (CEA), C.-H. Denarié and L. Zani (CEA) for helpful discussions. They are grateful to H. Immonen (Outokumpu) for providing a strand sample. The authors thank A. Bonasia, F. Diez, M. Laville, R. Matet, M.-C. Sogno and J.-L. Servais for invaluable technical support.

8 References

[1] Boutboul T, Denarié C-H, Charifoulline Z, Oberli L, Richter D. Critical current test facilities for LHC superconducting NbTi cable strands. LHC Project Report 520, CERN, Geneva, Switzerland, 2001.
[2] Ghosh A (BNL) and Rossi L (CERN), private communications.
[3] Ekin JW. Current transfer in multifilamentary superconductors. J. Appl. Phys. 1978;49(6):3406-3409.
[4] Dresner L. Distribution of current among the filaments of a multifilamentary superconductor close to the input leads. Cryogenics 1978;18(5):285-288.
[5] Adam JD, Boutboul T, Cavallari G, Charifoulline Z, Denarié C-H, Le Naour S, Leroy DF, Oberli LR, Richter D, Verweij AP, Wolf R. Status of the LHC superconducting cable mass production. IEEE Trans. Appl. Superconduct. 2002;12(1):1056-1062.
[6] Wolf R. Choice of some superconducting wire parameters for the ISR low-β section quadrupole. Internal Note ISR-MA/VB/RW/cb, CERN, Geneva, Switzerland, 1974.
[7] Duchateau J-L, Turck B, Krempasky L, Polak M. The self-field effect in twisted superconducting composites. Cryogenics 1976;16(2):97-102.
[8] Dresner L. Stability of Superconductors. New York: Plenum, 1995, chapter 3.